Ca^{2+}-Binding Site in *Rhodobacter Sphaeroides* Cytochrome *c* Oxidase†

Alex Lee,‡ Anna Kirichenko,§ T. Vygodina,§ Sergey A. Siletsky,§ Tapan Kanti Das,|| Denis L. Rousseau,|| Robert Gennis,*,‡ and Alexander A. Konstantinov§

Department of Biochemistry, University of Illinois at Urbana-Champaign, Urbana, Illinois 61801, A. N. Belozersky Insitute of Physico-Chemical Biology, Moscow State University, Moscow 119899, Russia, and Department of Physiology and Biophysics, Albert Einstein College of Medicine, 1300 Morris Park Avenue, Bronx, New York, New York 10461

Received March 5, 2002; Revised Manuscript Received May 14, 2002

ABSTRACT: Cytochrome *c* oxidase (COX) from *R. sphaeroides* contains one Ca^{2+} ion per enzyme that is not removed by dialysis versus EGTA. This is similar to COX from *Paracoccus denitrificans* [Pfitzner, U., Kirichenko, A., Konstantinov, A. A., Mertens, M., Wittershagen, A., Kolbesen, B. O., Steffens, G. C. M., Harrenga, A., Michel, H., and Ludwig, B. (1999) *FEBS Lett. 456*, 365−369] and is in contrast to the bovine oxidase, which binds Ca^{2+} reversibly. A series of *R. sphaeroides* mutants with replacements of the E54, Q61, and D485 residues, which form the Ca^{2+} coordination sphere in subunit I, has been generated. The substitutions for the E54 residue do not assemble normally. Mutants with the Q61 replacements are active and retain the tightly bound Ca^{2+}; their spectra are not perturbed by added Ca^{2+} or EGTA. The D485A mutant is active, binds to Ca^{2+} reversibly, like the mitochondrial oxidase, and exhibits the red shift in the heme *a* absorption spectrum upon Ca^{2+} binding for both reduced and oxidized states of heme *a*. The K_d value of 6 nM determined by equilibrium titrations is much lower than that reported for the homologous D477A mutant of *Paracoccus denitrificans* or for bovine COX ($K_d = 1-3\ \mu M$). The rate of Ca^{2+} binding with the D485A oxidase ($k_{on} = 5 \times 10^3\ M^{-1}\ s^{-1}$) is comparable to that observed earlier for bovine COX, but the off-rate is extremely slow ($\sim 10^{-3}\ s^{-1}$) and highly temperature-dependent. The k_{off}/k_{on} ratio (190 nM) is about 30-fold higher than the equilibrium K_d of 6 nM, indicating that formation of the Ca^{2+}-adduct may involve more than one step. Sodium ions reverse the Ca^{2+}-induced red shift of heme *a* and dramatically decrease the rate of Ca^{2+} binding to the D485A mutant COX. With the D485A mutant, 1 Ca^{2+} competes with 1 Na^+ for the binding site, whereas 2 Na^+ compete with 1 Ca^{2+} for binding to the bovine oxidase. This finding indicates that the aspartic residue D442 (a homologue of *R. sphaeroides* D485) may be the second Na^+ binding site in bovine COX. No effect of Ca^{2+} binding to the D485A mutant is evident on either the steady-state enzymatic activity or several time-resolved partial steps of the catalytic cycle. It is proposed that the tightly bound Ca^{2+} plays a structural role in the bacterial oxidases while the reversible binding with the mammalian enzyme may be involved in the regulation of mitochondrial function.

Cytochrome *c* oxidase (COX) is the terminal enzyme of mitochondrial and bacterial respiratory chains that reduces molecular oxygen to water and conserves the free energy of this exergonic reaction in the form of a transmembrane proton electrochemical potential gradient (reviewed, *1*−*3*). The catalytic core of the enzyme is comprised of four redox-active metal centers (heme *a*, heme a_3, Cu_A, and Cu_B). In addition, COX contains a number of nonredox metal ions, as revealed first by analytical methods (*4*−*8*) and confirmed subsequently by X-ray diffraction studies of the crystal structures (*9*−*13*). Zn^{2+} is bound to the nuclear-encoded subunit Vb in the bovine COX (*9*), and Mg^{2+} or Mn^{2+} is located at the interface between subunits I and II, close to the propionate groups of heme a_3 (*9*, *14*−*16*).

Recent crystallographic studies have drawn attention to the presence and potential significance of a "novel cation-binding site" in subunit I of COX, which can bind to Ca^{2+} or Na^+. Wikström and his collaborators first discovered that Ca^{2+} ions bind reversibly to mitochondrial COX, resulting in a small red shift (1−2 nm) of the absorption spectrum of the reduced heme *a* and competing with protons for the binding site (*17*, *18*). These observations were confirmed by other groups (*19*−*21*). The binding site was reported initially to be specific for Ca^{2+} and protons (*18*) (or hydronium cations as proposed in *21*). Subsequent studies showed that Na^+, at physiological concentrations, competes specifically with Ca^{2+} and protons for the binding site, although binding of Na^+ does not induce the spectral shift of heme *a* (*21*, *22*). The cation binding site has been

† Supported by National Institutes of Health Grants HL16101 (R.B.G.), GM54806 (D.L.R.), and GM 54812 (DLR), Civilian Research and Development Fund Award RC1-2063 (R.B.G. and A.A.K.); Russian Fund for Basic Research Grants 00-04-48262 (T.V.), 01-04-49330 (S.A.S.), and 99-04-48095 (A.A.K.), and Howard Hughes Medical Institute International Scholar Award 55000320 (A.A.K.).

* Corresponding author. Address: Department Biochemistry, UIUC, 600 S. Goodwin Ave, CLSL Building, Urbana (IL) 61801. Tel: (217) 333-9075. Fax: (217) 244-3186. E-mail: r-gennis@uiuc.edu.

‡ University of Illinois at Urbana-Champaign.

§ Moscow State University.

|| Albert Einstein College of Medicine.

[1] Abbreviations: COX, cytochrome *c* oxidase; TMPD, *N*,*N*,*N*′,*N*′-tetramethyl-*p*-phenylenediamine; RuBpy, tris−bipyridyl complex of Ru(II).

10.1021/bi020183x CCC: $22.00
Published on Web 06/21/2002

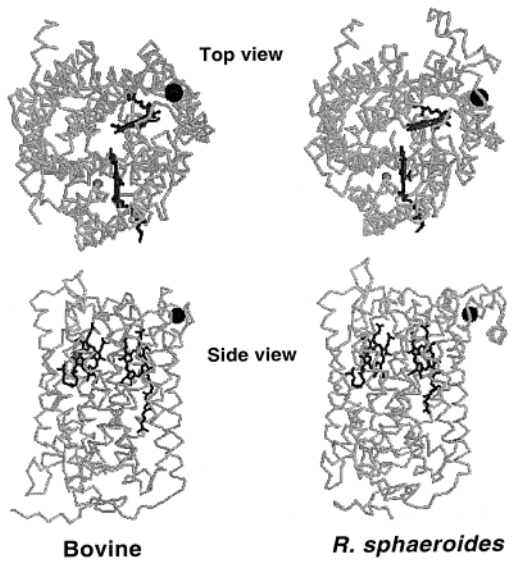

FIGURE 1: Location of the Ca^{2+} binding site in Subunit I of COX from bovine mitochondria and *Rhodobacter sphaeroides*.

identified with bound Na^+ in the X-ray structure of the bovine COX, whereas in the oxidases of *Paracoccus denitrificans* (*12*) and *Rhodobacter sphaeroides* (S.Iwata, personal communication), the site is complexed to Ca^{2+}. The cation binding site appears to be missing in the quinol oxidase members of the heme-copper superfamily (*23*) and in some bacterial cytochrome *c* oxidases such as ba_3 from *Thermus thermophilus* (*24*).

The positions of this site in Subunit I of the bovine and *R. sphaeroides* COX are shown in Figure 1. In both oxidases, the cation is located at the periplasmic periphery of the protein, close to heme *a*. There are some subtle differences between the structures of the bacterial and mitochondrial cation-binding sites, but generally, they are very similar. Despite the similarities between the structures of the cation-binding sites in bovine and bacterial COX, the Ca^{2+}-induced spectral shift is not observed in the oxidases from either *P. denitrificans* or *R. sphaeroides* (*22*). The explanation for this became apparent after the *P. denitrificans* oxidase was shown to retain bound Ca^{2+} even after prolonged incubation with excess EGTA (*25*). Since the endogenous Ca^{2+} is irreversibly bound to these bacterial enzymes, the addition of exogenous cation has no effect.

There are no significant effects of Ca^{2+} or Na^+ reported on the electron transfer or proton pumping activities of bovine COX, and the functional significance of the cation-binding site in COX is not known. The physical chemistry and mechanism of interaction between the cation and the binding site have not been explored in any detail. It is known that Ca^{2+} plays an important role in the structure and mechanism of heme-containing animal (*26*−*28*), bacterial (*29*, *30*), fungal (*31*−*33*), and plant peroxidases (*34*−*37*) as well as in Photosystem II (*38*). By analogy, it can be speculated that Ca^{2+} might participate in the oxygen/peroxide/water chemistry catalyzed by heme a_3. However, the cation-binding site in COX is clearly associated with heme *a*, not heme a_3.

Site-specific mutagenesis has been used in recent studies to provide an insight into the structure/function of the Ca^{2+}/Na^+/H^+ binding site. Mutants in the Ca^{2+}-binding site of

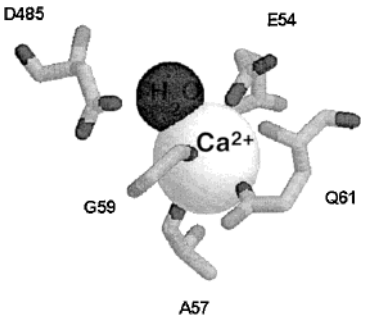

FIGURE 2: Coordination sphere of tightly bound Ca^{2+} ion in *R. sphaeroides* COX.

the *P. denitrificans* COX have been examined by two groups (*25*, *39*). The results are not in total agreement. Pfitzner et al. (*25*) showed that D477A mutation resulted in the loss of the tightly bound Ca^{2+} by the enzyme. In contrast to the wild-type COX, the D477A mutant demonstrated reversible binding of Ca^{2+}, with a K_d of about 1 μM and with a concomitant red shift of the absorption spectrum of heme *a*. Morover, competing effects of Na^+ or H^+ on Ca^{2+} binding were resolved. This behavior of the *P. denitrificans* D477A mutant is, thus, analogous to that of the native bovine COX. Interestingly, replacements of other residues in the Ca^{2+} coordination sphere of COX from *P. denitrificans*, such as Q63A or E56A, did not result in loss of the tightly bound Ca^{2+} (*25*). At the same time, Riistama et al. (*39*) reported that in the Q63A or E56Q mutants of *P. denitrificans* COX, the Ca^{2+}-induced shift can be observed, suggesting that the endogenous Ca^{2+} is lost in these mutants. However, the Ca^{2+} contents of their preparations were not determined (*39*).

Along with the *P. denitrificans* oxidase, the aa_3-type COX from *R. sphaeroides* has been widely used for elucidation of the COX structure and mechanism and is one of the best characterized enzymes within the heme-copper oxidase superfamily (*2*, *40*, *41*). Site-directed mutagenesis has been applied systematically to generate *R. sphaeroides* mutants in the functionally important domains, including the redox and nonredox metal-binding sites in the enzyme (*2*, *41*, *42*). The current work reports the initial step of our studies on the novel cation binding site in COX from *R. sphaeroides*. The structure of this site, based on the 3D model of the *R. sphaeroides* COX and kindly provided by Dr. So Iwata and Dr. Peter Brzezinski, is shown schematically in Figure 2. A series of mutants in the amino acid residues forming the Ca^{2+}-binding site in subunit I of the enzyme was generated. Replacement of D485 in the *R. sphaeroides* COX (homologous to D477 in *P. denitrificans*) results in loss of the tightly bound Ca^{2+}, whereas replacement of Q61 (a homologue of Q63 in *P. denitrificans*) does not. Accordingly, the addition of exogenous Ca^{2+} to EGTA-treated enzyme brings about a red shift of the heme *a* absorption spectrum in D485A but not in Q61(L,A). These data corroborate the results reported by Pfitzner et al. (*25*) with the *P. denitrificans* oxidase and confirm a specific role of the conserved aspartic residue D485 (D477 in *P.denitrificans*, D442 in bovine COX) in the cation binding site.

The D485A mutant COX from *R. sphaeroides* has been further exploited in this work to study in detail interaction of cations with the binding site. Reversible binding of Ca^{2+} with both the reduced and oxidized forms of D485A COX has been demonstrated. Using the red shift of the heme *a* α-

and γ-absorption bands as an indicator, we performed equilibrium titrations of Ca^{2+} binding with the use of appropriate Ca^{2+} buffers and and investigated the rapid kinetics of the reaction. Despite very high affinity (6 nM), Ca^{2+} binding to the site is surprisingly slow as compared to typical cellular Ca^{2+}-binding proteins such as calmodulins.

Na^+ competes with Ca^{2+} for the binding site in the D485A COX, as in bovine COX and the *P. denitrificans* D477A mutant oxidase. However, while 1 Ca^{2+} competes with 2 Na^+ in bovine COX (*22*), our data reveal 1:1 competition in the *R. sphaeroides* D485A mutant, indicating that one of the two Na^+ binding sites is lost in the mutant bacterial enzyme and pointing to the role of the conserved aspartate D442 (homologous to D477 in *P.denitrificans* and D485 in *R. sphaeroides*) in formation of this second Na^+-binding site in bovine COX.

Steady-state enzymatic turnover of the D485A mutant with or without bound Ca^{2+} did not reveal any modulation of the enzymatic activity of the enzyme by cation binding. Furthermore, Ca^{2+} binding has no affect on several time-resolved partial steps of the catalytic cycle in single-turnover experiments. The D485A mutant COX exhibits noticeable instability in both the reduced and oxidized states, losing heme absorption upon standing at room temperature, thus showing that D485 and Ca^{2+} contribute to maintaining the enzyme structure.

MATERIALS AND METHODS

Materials. All chemicals used were of reagent or analytical grade. Dodecyl-β-D-maltoside was obtained from Anatrace. Ni^{2+}−NTA agarose was obtained from Qiagen. Dithionite and horse heart cytochrome *c* (type VI) were from Sigma. DNA oligonucleotides were synthesized by the University of Illinois Biotechnology Center (Urbana, IL) or by Operon Technologies, INC.

Site-Directed Mutagenesis. D485A was constructed with QuickChange site-directed mutagenesis kit (Strategene). Q61L, Q61A, E54L, E54A, and E54L/Q61L were created by cassette mutagenesis. A unique restriction site BsrGI was introduced via QuickChange method to facilitate the mutagenesis. The mutant oligonucleotide cassettes were first phorphorylated then introduced into a region flanked by XbaI and BsrGI unique restriction sites. Double and triple mutants involving D485A (D485A/Q61L, D485A/E54L, D485A/Q61L/E54L, D485A/Q61A, and D485A/E54A) were constructed by digesting the single or double mutants with XbaI and EcoRI then inserting the mutant fragment into the corresponding DNA region on the D485A mutant plasmid. Silent mutations were created for all mutants to facilitate the mutagenesis process. All mutations were verified by DNA sequencing and checked for any mistakes that might have occurred elsewhere during amplification.

Protein Preparation. Wild-type and mutant cytochrome *c* oxidase, modified by a six-histidine affinity tag, was purified from *R. sphaeroides* as described previously (*43*). In addition, the enzyme was dialyzed against 50 mM HEPES adjusted to pH 8.0 with Tris−base, 0.02% dodecyl-β-D-matoside, and 4 mM EGTA for 10 h. The dialysis continued another 10 h in 50 mM HEPES adjusted to pH 8.0 with Tris−base and 0.02% dodecyl-β-D-maltoside.

Enzymatic Activity Assays. Cytochrome *c* oxidase activity was monitored spectrophotometrically by following oxidation of ferrocytochrome *c* at 550 nm using a Shimadzu UV-2101PC instrument. Reaction conditions were as follows: 50 mM potassium phosphate, pH 6.5, 0.02% dodecyl-β-D-maltoside, and 2−50 μM ferrocytochrome *c*.

Metal Content Analysis. Metal content was determined by using an Inductively-Coupled Plasma Atomic Emission Spectrometer at the Microanalytical Laboratory of the University of Illinois, Urbana, IL. Cytochrome aa_3 oxidase samples were approximately 20 μM in 50 mM HEPES adjusted with Tris−base to pH 8.0 and 0.1% dodecyl-β-D-maltoside. Three separate measurements were taken and averaged. Blank dialysis buffer was used as a control.

Cation-Induced Absorption Spectrum Shift. Experiments were carried out in 50 mM buffer (MES−Tris or HEPES−Tris, pH 8, if not indicated otherwise), containing dodecyl-β-D-maltoside (0.02−0.1%) and different concentrations of EGTA. In most experiments, the enzyme was prereduced with 5 mM ascorbate + 0.1 mM TMPD in the presence of 1 mM KCN. Care was taken to avoid Na^+ in the solutions. In particular, pH was adjusted with Tris−base rather than with KOH, which is significantly contaminated with sodium. Titrations of the absorption shift with Ca^{2+} were performed with calcium−EGTA buffer. Typically, increased amounts of Ca^{2+} were added to COX in a HEPES−Tris buffer, pH 8, containing 2−10 mM Tris−EGTA. Concentrations of free Ca^{2+} at given concentrations of EGTA, added Ca^{2+} and pH were calculated using the pK_a value for EGTA of 8.23 at pH 8 (*44*) either manually or with the use of Internet-available programs "Bound and Determined v. 4.35", written by S.Brooks, and "WinMAXC, v. 2.05", written by C.Patton, Stanford University.

Stopped-Flow Rapid Kinetics Measurements. Rapid mixing kinetics measurements were made with the Biosequential SX-17MV stopped-flow reaction analyzer from Applied Photophysics at 20 °C. For stopped flow on-rate studies, 5.2 μM enzyme in 50 mM HEPES−Tris, pH 8.0, 0.05% dodecyl maltoside, 1 mM KCN, 0.1 mM TMPD, 5 mM potassium ascorbate, and 0.1 mM EGTA were rapidly mixed with equal volume of solution containing 50 mM HEPES−Tris, pH 8.0, 0.05% dodecyl maltoside, 1 mM KCN, 0.1 mM TMPD, 5 mM potassium ascorbate, 0.1 mM EGTA, and varying amounts of Ca^{2+} (in excess over EGTA). The data were processed with Pro-K or MATLAB global analysis programs or imported into Origin 4 (Microcal) software for analysis and preparation of the figures.

Resonance Raman Measurements. The Raman spectroscopy measurements employed a CW He−Cd laser (Liconix, Santa Clara, CA) for the 441.6 nm excitation wavelength and a CW Kr-ion laser(Spectra Physics, Mountain View, CA) for the 413.1 nm excitation wavelength. The details of the procedure have been described elsewhere (*45*). The 2 mm path length sample cells were custom designed for strict anaerobic measurements and for recording both resonance Raman spectra and optical absorption spectra. Protein samples for the Raman measurements were10 μM in 50 mM Tris buffer, pH 8. Reduction of the oxidase samples was achieved by injecting a slight excess of an equimolar quantity of buffered dithionite solution into the Raman cell under strictly anaerobic conditions. To ensure the stability of the protein in a particular state, we measured optical spectra were measured for each sample before and after Raman measurements.

Table 1: Characteristics of the *R. Sphaeroides* COX Mutants in the Cation Binding Site

preparation	turnover (e^-/s)[a]	Ca content (mol/mol of COX)	spectral shift[b]
WT	1500	0.80 mol/mol	no
D485A	1600[a]	<0.1 mol/mol	yes
D485A/Q61A	1000	nd	yes
D485A/Q61L	1000	nd	yes
Q61L	800	0.85 mol/mol	no
Q61A	850	nd	no
E54L	inactive	nd	nd[c]
E54A/D485A	inactive	nd	nd[c]
E54L/ Q61L	inactive	nd	nd[c]
E54L /D485A/Q61L	inactive	nd	nd[c]

[a] The enzyme turnover rate was also measured with addition of 1 mM EGTA−Tris or 1 mM $CaCl_2$. No significant differences in the activity were observed. [b] The Ca^{2+}-induced spectral shift of heme *a* (addition of 10.5 mM Ca^{2+} in the presence of 10 mM EGTA−Tris) was measured in 50 mM HEPES−Tris buffer, pH 8.0, with 0.1% dodecyl maltoside with 2 μM COX reduced by 5 mM ascorbate and 0.1 mM TMPD in the presence of 1 mM cyanide. [c] Abnormal absorption characteristics of heme *a*.

Electrometric Measurements. Time-resolved electrometric measurements of membrane potential generation by phospholipid vesicle reconstituted COX were carried out as earlier (*46*−*48*) using the Tris−bipyridyl complex of Ru(II) (RuBpy) as a photoactive electron donor to the Cu_A redox center of COX (*49*).

RESULTS

In COX from *R. sphaeroides*, Ca^{2+} is coordinated by six oxygen atoms (Figure 2). Five of the ligands are provided by amino acid residues in the cytoplasmic loop connecting transmembrane helixes I and II. Of these five ligands, two bonds (to a carboxylate oxygen and the peptide carbonyl) are donated by E54, while Q61 coordinates Ca^{2+} via the amide oxygen. Two more bonds are provided by peptide carbonyls of G59 and A57. The sixth position in the Ca^{2+} coordination sphere is occupied by an immobilized water molecule (cf. *25*) which, in turn, is hydrogen bonded to D485. The structure of the binding site is almost identical to that described for COX from *P. denitrificans*, except that in the latter it is histidine rather than alanine in position 59 (residue 57 in *R. sphaeroides*) that donates one of the backbone carbonyls (*12*, *25*).

Mutants were generated with replacements of each of the three amino acid residues (D485, E54 and Q61) whose side chains participate in Ca^{2+} binding. In addition, double and triple mutants in those residues were obtained. Some characteristics of the mutants are summarized in Table 1.

The wild-type enzyme contains about 1 equiv of tightly bound Ca^{2+} after extensive dialysis versus EGTA, in agreement with the data obtained with COX from *P. denitrificans* (*12*, *25*). The mutant in which E54 was replaced by leucine (E54L) did not assemble properly, and multiple mutants containing an E54L or E54A substitution (E54A/D485A, E54L/Q61L, E54L/D485A/Q61L) also did not assemble properly, were devoid of enzymatic activity, and revealed strongly modified spectral characteristics. These E54 mutants were not further investigated. The mutants in Q61 and D485 have activity and spectroscopic characteristics similar to those of the wild-type COX. The Q61L mutant retains bound Ca^{2+}, which could not be removed by EGTA,

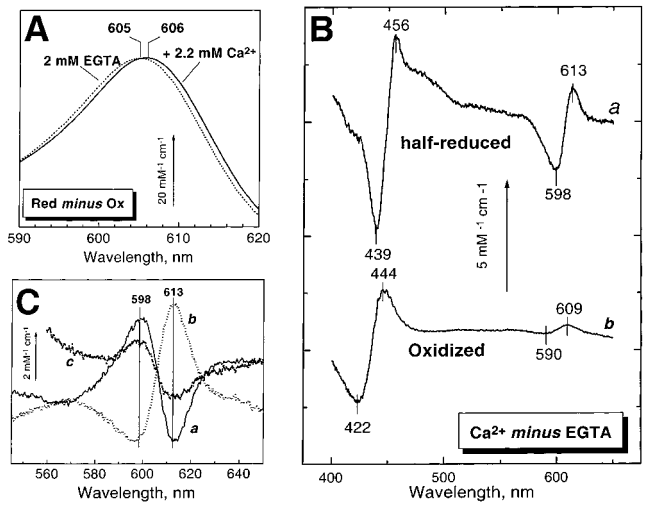

FIGURE 3: Absorption shift induced by Ca^{2+} and EGTA in the D485A mutant of COX from *R. sphaeroides*. Experiments have been carried out in standard 1 cm cuvettes. The D485A COX, in 50 mM Tris−MES buffer, pH 8, with 0.05−0.1% dodecyl maltoside was reduced by 5 mM ascorbate + 0.1 mM TMPD in the presence of 2 mM KCN (except for trace b in panel B, where 100 μM K^+−ferricyanide and 4 μg/mL of poly-L-lysine have been added to provide for the oxidized cyanide-inhibited complex). (A) Reduced-minus-oxidized spectra of D485A in the presence of 2 mM EGTA (dotted line) and after subsequent addition of excess Ca^{2+} (solid line). (B) Difference spectra of the Ca^{2+}-induced shift. The difference spectra show the effect induced by addition of 10.5 mM Ca^{2+} to COX preincubated in the presence of 10 mM Tris−EGTA. COX concentration was 2.0 μM for spectrum a and 4.1 μM for spectrum b. The spectra are normalized to concentration of the enzyme. (C) Reversibility of the heme *a* red shift (a). Difference spectrum induced by the addition of 2 mM Tris−EGTA to the D485A oxidase (1 μM) showing the reversal of the red shift induced by adventitious Ca^{2+}; (b) spectrum a was taken as baseline, and Ca^{2+} was added to a final concentration of free Ca^{2+} of 61 nM; (c) spectrum b was taken as a baseline and 50 mM Na^+ (25 mM Na_2SO_4) was added.

and accordingly, the Q61(L,A) mutants do not display the Ca^{2+}-induced red shift. These findings agree with the data of Pfitzner et al. (*25*) regarding the *P. denitrificans* Q63A COX (equivalent to Q61A in *R. sphaeroides*) but disagree with ref *39*, which describes a Ca^{2+}-induced shift for the same Q63A mutant of *P. denitrificans* COX.

In contrast to Q61L, the mutants of the *R. sphaeroides* oxidase with the D485 replacement show substantial loss of Ca^{2+} upon dialysis versus EGTA (Table 1). Accordingly, after removal of the endogenous Ca^{2+}, the D485 COX displays a Ca^{2+}-induced red shift of the absorption spectrum.

Ca^{2+}-Induced Red Shift of the Spectrum of the D485A Mutant.

Figure 3 shows the absorption changes induced by the addition of Ca^{2+} to D485A COX from *R. sphaeroides* pretreated with EGTA to remove the endogenous Ca^{2+}. A 1 nm red shift in the position of the α-absorption band induced by Ca^{2+} can be directly seen in the reduced-minus-oxidized spectrum (Figure 3A), but the effect is much better revealed by the difference spectra of the cation-induced absorption changes (Figure 3B,C). The Ca^{2+}-induced absorption changes are observed with COX, in which heme *a* is reduced (Figure 3B, curve a) or oxidized (Figure 3B, curve b), both in the α-band and in the Soret. The difference spectra are typical of a small red shift of the heme *a* spectrum. In the case of the reduced heme *a* (curve a), the Ca^{2+}-induced absorption

changes are similar to those previously described for bovine COX and for mutant forms of the *P. denitrificans* enzyme (*18*, *22*, *25*, *39*). The differences in the line shape of the Ca^{2+}-induced spectral changes between the reduced and oxidized samples are in agreement with attribution of the spectral perturbation to heme *a*. The Ca^{2+}-induced red shift of heme *a* can be fully reversed by the addition of excess EGTA (Figure 3C, curve a) and then restored by adding more Ca^{2+} (Figure 3C, curve b).

Studies of Ca^{2+} Binding under Equilibrium Conditions. The Ca^{2+}-induced absorption changes in the *R. sphaeroides* D485A COX develop at concentrations of the cation much lower (nM range) than those observed previously with either the bovine oxidase or with the *P. denitrificans* D477A mutant (corresponding to D485A in *R. sphaeroides*). Consequently, the cation binding site of D485A appears to be saturated by adventitious Ca^{2+} even in the absence of added Ca^{2+} (e.g., Figure 3C, spectra a and b). Therefore, equilibrium titrations of Ca^{2+} binding to the *R. sphaeroides* D485A required the use of a high-affinity Ca^{2+} buffer, such as EGTA (pK_{Ca} 8.23 at pH 8, *44*). Typically, increased amounts of Ca^{2+} were added to COX in HEPES−Tris buffer, pH 8, containing 2−10 mM EGTA.

Figure 4A shows the absorption changes induced in the cyanide-inhibited ascorbate+TMPD-reduced D485A COX by the addition of 1.8 mM $CaCl_2$ in the presence of 2 mM EGTA (21 nM free calcium, final concentration). The response develops rapidly enough and the extinction at 612 minus 598 nm reaches a value of ca. 4 mM^{-1} cm^{-1}, close to the maximal size of the response observed with the bovine or *P. denitrificans* enzymes (*22*, *25*, *39*). No absorption changes were observed under these conditions with bovine COX (K_d for Ca^{2+} binding of 1.3 μM, *22*). At concentrations of free Ca^{2+} below ~5 nM, the development of the absorption changes was much slower and could require tens of minutes to reach the equilibrium state. Representative difference spectra in the α-band obtained with increasing concentrations of free calcium in the nM range are given in Figure 4B, and Figure 4C shows a complete titration curve. The specific absorption changes reach saturation at less than 40 nM of free Ca^{2+}. The data fit a model in which there is a single site with a K_d of 6 nM and ΔA_{max} of 4.4 mM^{-1} cm^{-1}. There may be some minor phase (ca. 20−25%) with even higher affinity for Ca^{2+}. However, the lower concentration range is difficult to study with the EGTA buffer due to the slow rate of development of the absorption changes and because the reversibility of the changes is difficult to verify. Therefore, the possibility of a higher affinity binding site was not pursued.

Kinetics of Ca^{2+} Binding. Association Rate Constant, k_{on}. The rate constant of Ca^{2+} binding with D485A COX was determined with the aid of rapid-mixing techniques. Figure 5A shows the time evolution of the spectral changes observed upon rapid mixing of the mixed-valence D485A COX with 70 μM $CaCl_2$. The four representative spectra shown have been extracted from the full spectra/time surface (1600 full-spectrum scans/32.8 s), and the data have been normalized to the concentration of the enzyme. The difference spectra show a line shape typical of the Ca^{2+}-induced red shift of heme *a* in both the Soret and α-bands, with isobestic points at 448 and 605 nm, respectively. Figure 5B shows the kinetics of the absorption changes in the α-band extracted from the same data set. The curve is fit well by a single exponent with τ of 3.6 s. The same rate constant is obtained if the kinetics of the absorption changes in the Soret band

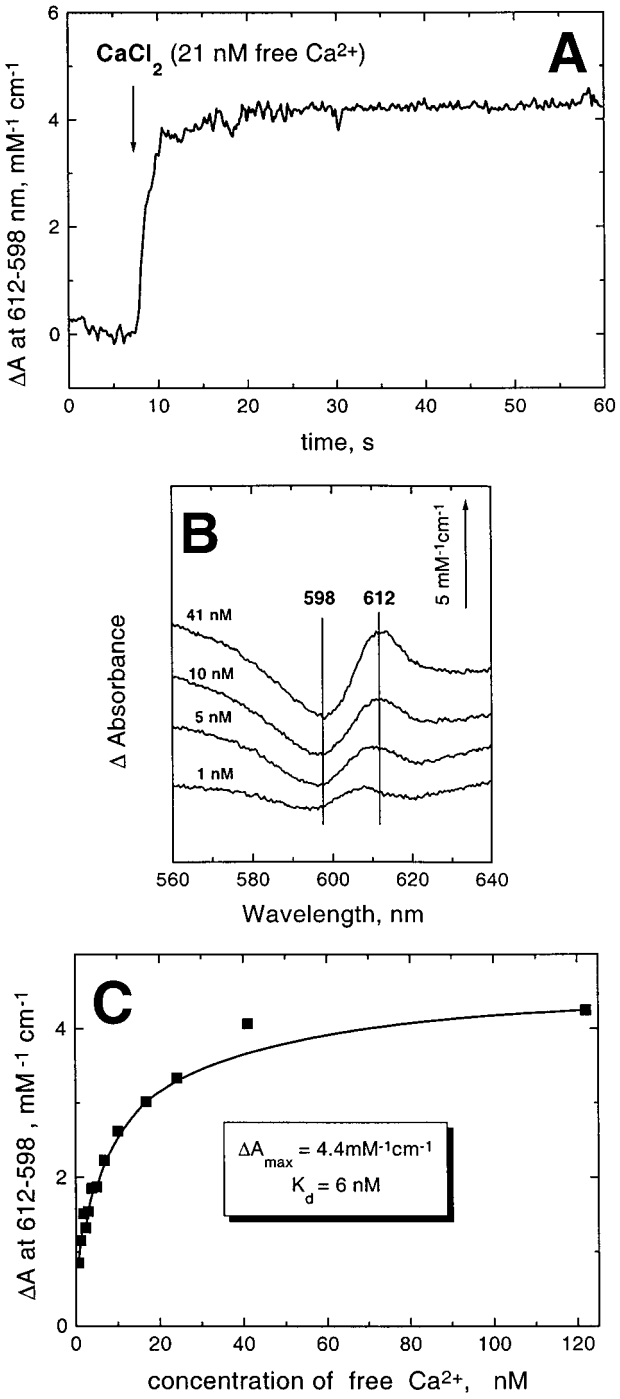

FIGURE 4: Spectral shift of heme *a* in D485A COX induced by nanomolar concentrations of free Ca^{2+}. Experiments were carried out with an SLM-Aminco 2000 spectrophotometer in 50 mM Tris−MES buffer, pH 8, containing 0.05% dodecyl maltoside and 2 mM EGTA. The D485A mutant (1 μM) was prereduced by 5 mM ascorbate and 0.1 mM TMPD in the presence of 1 mM KCN. Titrations were carried out by adding increasing concentrations of Ca^{2+}. (A). Time-dependence of the development of the spectral shift of heme *a* induced by 21 nM free Ca^{2+} (1.8 mM Ca^{2+} added). (B) Representative difference spectra recorded during equilibrium titrations of the heme *a* spectral shift with Ca^{2+} /EGTA buffer. (C) Concentration dependence of the heme *a* spectral shift induced by Ca^{2+}. The data have been fit with a single-site binding curve with the indicated parameters.

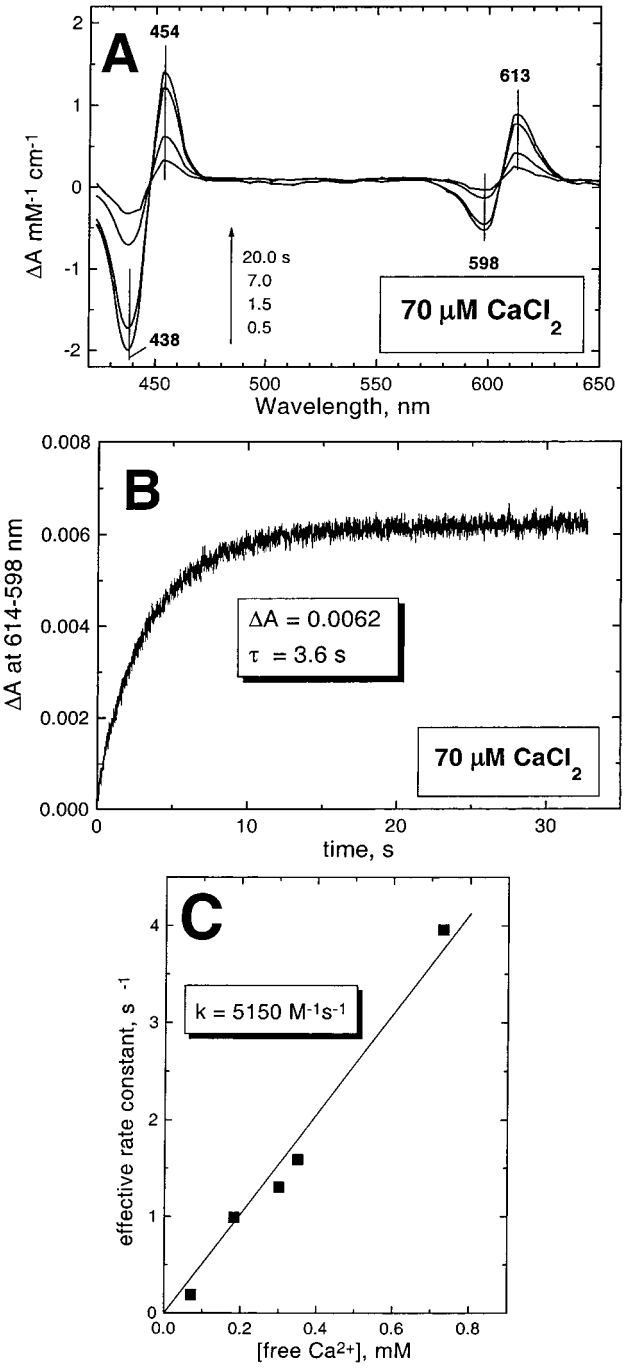

FIGURE 5: Rapid kinetics of Ca^{2+} binding to the D485A COX from *R. sphaeroides*. Experiments were performed in a rapid-mixing diode array spectrophotometer as described in the text. The final enzyme concentration after mixing was 2.6 μM. Free Ca^{2+} concentration after mixing, 70 μM. 1600 evenly distributed scans were collected during the observation period of 32.8 s. The first scan in the series was taken as a baseline subtracted from all subsequent curves to obtain the difference spectra of the Ca^{2+}-induced changes. The extent of the specific Ca^{2+}-induced absorption changes in the first scan is negligible. (A) Representative difference spectra extracted from the spectrum/time surface. The spectra have been adjusted to the same zero line by the absorption at 630 nm to eliminate baseline shifts. (B) Kinetics of the time development of the absorption shift. The trace has been extracted from the same data set as in panel A. (C) Concentration dependence of the effective rate constant of Ca^{2+} binding to the D485A COX. The experiment shown in panels A and B was repeated at different concentrations of $CaCl_2$, varying the observation period. The line drawn through the points was obtained by a linear fit of the data.

(e.g., at 453 minus 438 nm, not shown) is analyzed for the data set.

Rapid mixing experiments were repeated at different concentrations of Ca^{2+}. For each data set, the rate constant of Ca^{2+} binding was determined as shown in Figure 5B. The results are given in Figure 5C. The effective rate constant of the Ca^{2+}-induced spectral shift development grows linearly with increased Ca^{2+} concentration, yielding the second-order rate constant of 5.15×10^3 M^{-1} s^{-1}. This value is not radically different (about 5.5-fold lower) from the second-order rate constant of 2.8×10^4 M^{-1} cm^{-1} as determined earlier by A.Kirichenko and T.Vygodina for Ca^{2+} interaction with bovine COX (*50*, *51*). It is, however, 10^4-10^5-fold slower than typical association rate constants for Ca^{2+} binding to intracellular Ca^{2+}-binding proteins with similar affinities for the Ca^{2+}, e.g., calmodulins or calbindins (cf. *52*, *53*, and references therein).

Dissociation Rate Constant, k_{off}. As shown above, the spectral shift of heme *a* induced by Ca^{2+} binding with the D485A mutant can be fully reversed by excess EGTA (Figure 3C). We have studied the kinetics of the spectral shift reversal. Rapid mixing of 5 mM EGTA (final concentration) with the enzyme reduced aerobically by ascorbate + TMPD in the presence of KCN and preloaded with 50 μM Ca^{2+} is followed by extensive, slow absorption changes in the Soret and visible ranges (Figure 6A). However, the difference spectra of the changes are not identical with those expected from simple reversal of the Ca^{2+}-induced shift and are likely to report several processes. Moreover, there are significant spontaneous slow spectral changes observed with the D485A enzyme even in the absence of EGTA (Figure 6B). These spontaneous spectroscopic changes show a gradual loss of absorption in both the α- and Soret bands and appear to result from some instability of the mutant oxidase. Similar instability has been observed also with the oxidized enzyme (not shown). Overlapping the EGTA-independent "spontaneous" absorption changes is the spectral perturbation resulting from the reversal of the Ca^{2+}-induced shift (Figure 6A). The latter can be clearly resolved by subtracting the spontaneous time-dependent changes occurring in the absence of EGTA from those observed with EGTA (Figure 6C). To extract the kinetics of Ca^{2+} dissociation from the overall absorption changes, we examined the reaction using several different modes of spectrophotometric measurements. First, a stopped-flow diode-array spectrophotometer was used to collect a large spectrum/time data surface in a single-beam mode of operation (as in Figure 6). This surface was processed subsequently by different routines to extract the absorption changes specific for Ca^{2+} dissociation. Second, an Aminco-SLM-2000 split-beam/dual wavelength instrument was employed to collect the spectrum/time surface in a split-beam mode with manual mixing. Since the rate of absorption changes is slow, it is possible to sequentially record difference spectra in the entire 350−700 nm range, requiring about 2 min per spectrum. In this mode of measurements, the spectra are taken versus a reference cell containing the same reaction mixture but without EGTA, which eliminates contribution of the spontaneous changes during the measurements already. Third, the rate of Ca^{2+} dissociation was measured using the Aminco-SLM instrument in a dual-wavelength mode (612 nm minus 598 nm). This minimizes the problems due to slow baseline drifts and

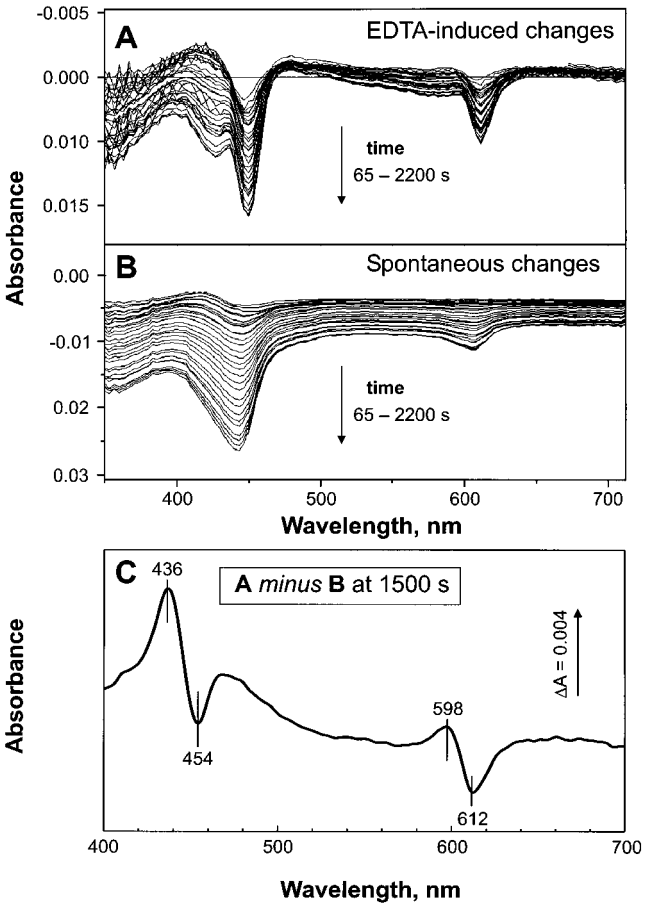

FIGURE 6: Reversal of the Ca^{2+}-induced spectral shift of heme *a* by EGTA addition to the D485A oxidase. (A) Evolution of spectral changes following mixing of EGTA with Ca^{2+}-loaded D485A COX. 5.2 μM D485A COX (2.6 μM final concentration after mixing) in 50 mM HEPES−Tris, pH 8.0, 0.05% dodecyl maltoside, 1 mM KCN, 5 mM potassium ascorbate, 0.1 mM TMPD, and 50 μM $CaCl_2$ was rapidly mixed in a stopped-flow apparatus with an equal volume of the same buffer, but containing also 5 mM EGTA and no $CaCl_2$. The absorption changes were followed for 2000 s in a diode array mode collecting 1600 spectra. Each 50th spectrum of the data set is shown. (B) Spontaneous time-dependent spectral changes observed in the absence of EGTA. The experiment was performed was the same as that in panel A, but the buffer in the second syringe was the same as that in the syringe with COX (i.e., containing 50 μM $CaCl_2$ and no EGTA). (C) Absorption difference between the samples in the experiments shown in panels A and B 1500 s after mixing.

nonspecific absorption changes associated with enzyme instability that are more difficult to avoid in case of slow reactions using a single-beam mode of operation. Having compared these three different approaches, it was found that the kinetics of the absorption changes ($A_{612-614}$ minus A_{598}), whether extracted from the diode array-obtained data sets or recorded in a dual-wavelength mode, is fairly specific for the reversal of the Ca^{2+} shift induced by EGTA. These data have been used for evaluation of the Ca^{2+}-dissociation rate.

With the freshly isolated COX, the off reaction is essentially monophasic with a rate constant of 0.0005−0.001 s^{-1} as measured for different preparations (Figure 7A, trace a). This off rate is 10^3-fold slower than that for Ca^{2+} dissociation from the bovine COX (k_{off} of 0.5 s^{-1}; *50*, *51*) and 10^4-10^6 slower than the off rates for different sites in calmodulin (*52*). A similar extremely slow rate has also been measured for Ca^{2+} dissociation from the oxidized D485A

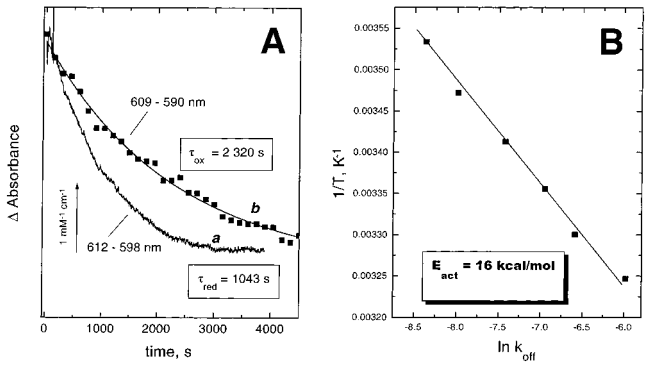

FIGURE 7: Kinetics of the EGTA-induced dissociation of Ca^{2+} from the binding site in the D485A COX. (A) Typical kinetics traces at 20 °C. Curve a: D485A COX (1 μM) in 50 mM MES−Tris buffer, pH 8.0, and 0.05% dodecyl maltoside was reduced with 5 mM ascorbate and 100 μM TMPD in the presence of 2 mM KCN. At the zero time, 2 mM EGTA was added to reverse the spectral shift induced by endogenous Ca^{2+}. The kinetics of the reaction was followed in a stirred 1 cm cuvette in an SLM-Aminco 2000 spectrophotometer operating in a dual-wavelength mode. Curve b: Same as curve a, but the experiment was done with aerobically oxidized D485A COX (~3 μM), and the absorption changes (cf. Figure 3B, spectrum b) were monitored by sequential recording of the spectra on an Aminco-SLM every 150 s. The two curves are given normalized to the maximal ΔA value. The scale bar refer to curve a. (B) Temperature dependence of the Ca^{2+} off rate. The experiment shown in panel A, curve a has been repeated at temperatures 10−35° C.

(Figure 7A, trace b). The rate of Ca^{2+} dissociation shows quite a strong temperature dependence of 16 kcal/mol (Q_{10} 2.5−2.7) (Figure 7B), similar to that observed for Ca^{2+} release from calmodulin (*52*). This slow off rate appears to be a major factor responsible for the much tighter binding of Ca^{2+} to the *R. sphaeroides* D485A enzyme compared to the bovine oxidase. Dissociation of Ca^{2+} from the wild-type *R. sphaeroides* enzyme, reduced or oxidized, is never observed.

If Ca^{2+} binding with COX were a simple single-step process, the equilibrium dissociation constant for the ligand should equal the ratio of the off and on rate constants: $K_d = k_{off}/k_{on}$. In bovine COX, the K_d values determined by equilibrium titrations and kinetic measurements are indeed close to each other (Kirichenko and Vygodina, unpublished, *51*). This is not the case for the *R. sphaeroides* D485A COX. Taking a value of 5.15×10^3 M^{-1} s^{-1} for the second-order k_{on} for Ca^{2+} binding (Figure 5C) and the off rate constant of 10^{-3} s^{-1} (Figure 6C), we obtain the value for the equilibrium dissociation constant K_d = 190 nM. This is about 30-fold higher than the value of 6 nM determined by equilibrium titrations. Such a difference cannot be accounted for by an inaccuracy in the kinetic measurements or data analyses. It is, therefore, possible that binding of Ca^{2+} with the mutant bacterial COX involves more than one step so that the kinetically measured rates of spectral changes in the on and off reactions reflect rate constants of partial steps that do not give the overall k_{on} and k_{off} of Ca^{2+} binding (see Discussion).

Effect of Sodium Ions on the Interaction of the D485 Oxidase with Ca^{2+}. Studies with bovine COX showed that Na^+ ions compete with both Ca^{2+} and protons for binding to the enzyme. Sodium reverses the red shift of heme *a* induced by either Ca^{2+} or protons but does not perturb itself the spectrum of heme *a* (*21*, *22*). The inhibitory effect of

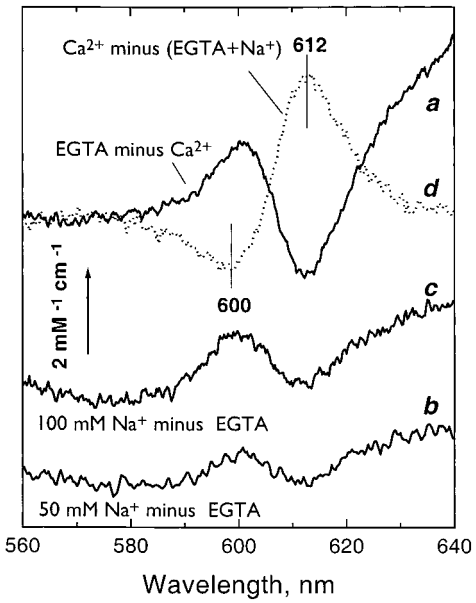

FIGURE 8: Na^+-induced blue shift in the EGTA-treated D485A oxidase. Basic conditions were the same as those in Figure 7A, trace a. (a) The difference spectrum induced by the depletion of endogenous Ca^{2+} induced by the addition of EGTA to the mixed-valence enzyme. The kinetics of the effect is shown in Figure 7. Curve a has been taken as a baseline for the difference spectra b−d. (b and c) Spectral perturbation induced by the addition of Na_2SO_4 to EGTA-treated COX to a final salt concentration of 25 and 50 mM, respectively. The changes took about 20 min for completion. (d) Ca^{2+} was added to the cuvette to a final concentration of free Ca^{2+} of 61 nM.

Na^+ on Ca^{2+} binding with the *P.denitrificans* mutants in the Ca^{2+} site has also been reported (*25*, *39*). As expected, Na^+ does not affect the absorption spectrum of the wild-type oxidase from *R. sphaeroides*. When added to the D485A mutant equilibrated with Ca^{2+}−EGTA buffer (60 nM free Ca^{2+}, ca. $10\times K_d$), Na^+ ions cause a blue shift of absorption spectrum (Figure 3C), partially reversing the red shift induced by Ca^{2+}. The kinetics of the development of the Na^+-induced blue shift is characterized by the same τ value of $\sim 10^3$ s that is characteristic of the EGTA-induced blue shift (data not shown). Hence, it is likely that reaction is limited in both cases by the same process of Ca^{2+} dissociation from the binding site.

It was recently reported that Na^+ itself induces a red shift in the Ca^{2+}-depleted E56Q mutant of the *P.denitrificans* (*39*). We were not able to observe such an effect in the D485A mutant of the *R. sphaeroides* oxidase. Figure 8 shows the results of an experiment in which Ca^{2+} is first depleted from the D485A mutant, followed by the addition of Na^+. Removal of endogenous Ca^{2+} by excess EGTA gives rise to a substantial blue shift of the heme *a* absorption (Figure 8, spectrum a). Under these conditions, the addition of 50−100 mM Na^+ does not induce a red shift of heme a (cf. *39*) but, rather, a further blue shift of heme a spectrum (traces b and c). Similar data have been obtained with the equivalent mutation (D477A) in the *P. denitrificans* oxidase (Kirichenko, unpublished). Presumably, in the EGTA-treated COX, the cation binding site is partially occupied by protons, resulting in a red shift of the heme *a* spectrum in a fraction of the enzyme. The binding of Na^+ reverses this partial red shift by displacing the proton(s) but does not itself perturb the spectrum of heme *a*. In the bovine oxidase, the pK_a of the group responsible for the protonation-induced red shift of heme *a* is around pH 6 (*18*), so no Na^+-induced blue shift is observed at pH 8 (*22*). It is possible that in the *R. sphaeroides* oxidase, the pK_a of the protonatable group is higher than that in bovine oxidase, as may also be the case for the *P. denitrificans* E56Q mutant (*39*).

Competition between Ca^{2+} and Na^+ ions for binding to the oxidase has been studied in more detail following the kinetics of absorption changes of the D485A mutant induced by 300 μM Ca^{2+} at different concentrations of Na^+ in the buffer. As shown in Figure 9A, addition of 20 mM Na^+ drastically reduces the rate of Ca^{2+} binding to the enzyme. The same concentration of K^+ has little effect; the minor deceleration observed is possibly due to cross-contamination of the K^+ solution with Na^+. Thus, the inhibition of Ca^{2+} binding is not induced simply by ionic strength and is specific for sodium ions.

Interestingly, the K_d for Ca^{2+} binding to the bovine enzyme shows a parabolic, rather than linear, dependence on Na^+ concentration indicating competition of one Ca^{2+} with two sodium ions (*22*). The Na^+-dependence of the k_{on} rate constant for Ca^{2+} binding to the D485A mutant was examined (Figure 9). At the high concentration of Ca^{2+} used in this study (300 μM Ca^{2+}; 5000-fold K_d), increasing the Na^+ concentrations up to 50 mM did not significantly reduce the amplitude of the response but induced a progressive decrease in the binding rate. The plot of the time-constant of the reaction versus Na^+ concentration is not parabolic, but linear (Figure 9B). In the same concentration range, the presence of Na^+ has no significant influence on the rate of EGTA-induced dissociation of Ca^{2+} from the binding site in D485A (data not shown). Therefore, the effect of Na^+ on the k_{on} of Ca^{2+} binding is likely to imply a proportional effect on the equilibrium dissociation constant, K_d . These results may indicate that one of the two Na^+ binding sites found in bovine COX is lost in the *R. sphaeroides* D485A enzyme.

Resonance Raman Spectra. As proposed in ref *39*, Ca^{2+} binding might perturb the spectral characteristics of heme *a* by affecting the strength of a hydrogen bond between the formyl group of heme *a* and a conserved arginine residue (R52 in *R. sphaeroides*, R54 in *P. denitrificans*). This possibility was experimentally tested by determining the stretching frequency of the formyl group in the wild type and D485A oxidases. Experiments were performed with both the reduced and oxidized enzyme with laser excitation in the Soret band (441 or 413 nm, respectively). There are subtle differences between the resonance Raman spectra of the wild-type oxidase and the D485A mutant. There is an increase in intensity of the low-spin marker bands at 1503 (ν_3) and 1585 (ν_2) relative to the high-spin marker at 1569 cm^{-1} in the oxidized state (Figure 10B), broadening of the redox-state marker band at 1354 cm^{-1}, and an increase of intensity around the 1470 cm^{-1} band in the reduced enzyme (Figure 10A). However, these changes are Ca^{2+}-independent and may report some general perturbation of the enzyme structure induced by the mutation (cf. *45*). The stretching frequency of the heme *a* formyl group in the resonance Raman spectrum of the reduced enzyme at about 1611 cm^{-1} is found at 1609 cm^{-1} in the Ca^{2+}-supplemented D485A mutant and shifts slightly (by 1 cm^{-1}) to higher frequencies upon removal of Ca^{2+} by EGTA (Figure 10A). This can be compared to a

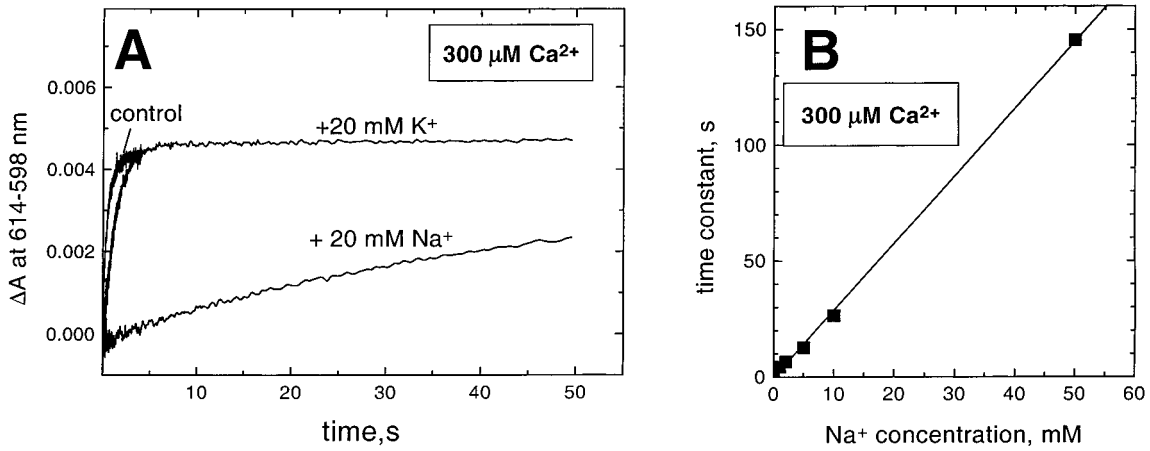

FIGURE 9: Effect of Na^+ ions on the kinetics of Ca^{2+} binding to the D485A oxidase. (A) Representative kinetic traces. Rapid mixing experiments have been performed essentially as in Figure 5 at a Ca^{2+} concentration of 300 μM in the presence of 20 mM NaCl or 20 mM KCl. The final enzyme concentration was 2.6 μM. 500 spectral scans were collected in a 50 s observation interval with a logarythmic sweep of the aquisition time points. The control trace has been recorded during a 4 s observation period with an even distribution of the time points. (B) Effect of Na^+ on the time constant of the binding of 300 μM Ca^{2+} with the D485A oxidase. The experiment in Figure 9A was repeated at different concentrations of Na^+. The data are fit to a linear dependence.

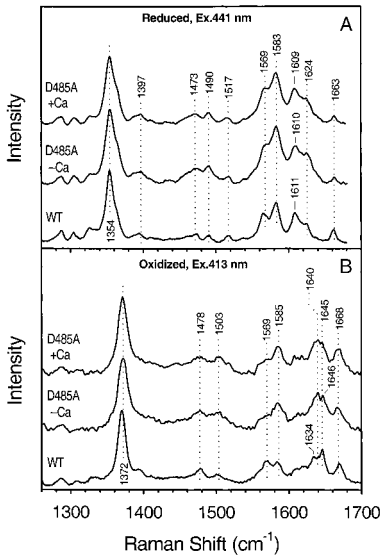

FIGURE 10: Resonance Raman spectra of dithionite-reduced (A) and air-oxidized (B) D485A oxidase. The excitation wavelengths for the reduced and oxidized samples were 441 and 413 nm, respectively. See the text for further details.

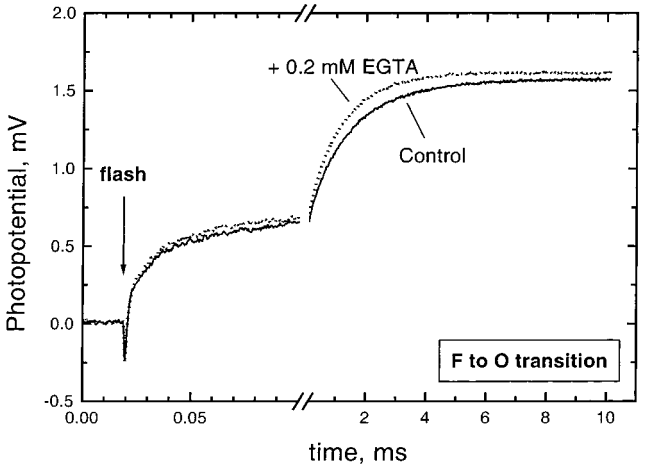

FIGURE 11: Time dependence of the generation of membrane potential using D485A oxidase reconstituted in phospholipid vesicles. Laser-flash-induced photoreduction of phospholipid vesicle-reconstituted D485A COX with RuBpy was monitored electrometrically. Experiments were carried out in the buffer containing 5 mM Tris−acetate buffer, pH 8, 10 mM aniline and 40 μM RuBpy. Before flashing the sample, the oxidase was converted to the ferryl oxo state by the addition of 1.6 mM H_2O_2.

frequency shift of 5 cm^{-1} to low energy induced by the R52K replacement, which increases the hydrogen bonding to the formyl group, inducing a 4 nm red shift of the heme *a* α-band (*45*). The R52A mutation results in a 14 cm^{-1} shift to higher frequencies, corresponding to the loss of the hydrogen bond to the formyl group, and a blue shift of the of heme *a* absorption peak by 10 nm is observed. Thus, the 1 cm^{-1} Ca^{2+}-induced low-frequency shift in D485A formyl stretch is in the expected direction and is consistent with the proposal in (*39*). However, as the magnitude of the shift is about the error of the measurements, a definitive conclusion cannot be based on these data.

Electrometric Measurements Show No Effect of Ca^{2+} on the Intraprotein Electron and Proton-Transfer Steps. The cytochrome *c* oxidase cation binding site is missing in the quinol oxidase members of the heme−copper oxidase "superfamily" (*23*). On this basis, it was proposed that bound Ca^{2+} may be specifically required for electron transfer among Cu_A, a redox center specific for cytochrome *c* oxidases, and heme *a* (*39*). We examined the effect of Ca^{2+} on the kinetics of intraprotein electron and proton transfer in the *R. sphaeroides* D485A oxidase with/without bound Ca^{2+}. Figure 11 shows the time course of the membrane potential generation by the *R. sphaeroides* enzyme initiated by rapid single-electron photoreduction of the ferryl-oxo state of COX (compound F) to the oxidized form. There were no significant differences between the results obtained with D485A enzyme loaded with Ca^{2+} or depleted of Ca^{2+} (Figure 11) or between D485A and wild-type oxidase (not shown). The rapid electrogenic phase associated with $Cu_A \rightarrow$ heme *a* electron transfer is not dependent on Ca^{2+}. There is a slight acceleration of the slow part of the photoelectric response induced by EGTA in both the wild-type and D485A oxidases. This effect may be due to EGTA-induced removal of adventitious metal cations causing a change in the membrane surface pH, as previously observed in bacteriorhodopsin (*54*, *55*), and at

the output proton channels of the bacterial photosynthetic reaction center complexes (*56*).

DISCUSSION

"Tightly Bound" Ca^{2+} in Bacterial COX. Cytochrome *c* oxidase from *R. sphaeroides* contains one tightly bound Ca^{2+} ion per enzyme molecule that cannot be removed by prolonged dialysis versus EGTA. In this respect, COX from *R. sphaeroides* is similar to the oxidase from *P. denitrificans* (*12*, *25*) and different from mammalian COX, which binds Ca^{2+} reversibly, and easily loses the cation upon the addition of a slight molar excess of EGTA (*17*, *18*, *20*−*22*).

The inability of EGTA to remove Ca^{2+} from the bacterial oxidases could be a true equilibrium situation reflecting a very high affinity of Ca^{2+} for the binding site in the bacterial oxidases (higher than that for EGTA) or, alternatively, might indicate that the cation is kinetically trapped (caged) in the binding site. Our data indicate that both factors may contribute to the "tight binding" of Ca^{2+} with the *R. sphaeroides* oxidase.

Affinity of the *R. sphaeroides* D485A oxidase for Ca^{2+} ($K_d \sim 6$ nM) is surprisingly high as compared either to that of bovine COX (*22*) or to those of various mutants of the *P. denitrificans* oxidase (*25*, *39*) (K_d values in the 1−100 μM range). This difference in the affinities between the mutant *R. sphaeroides* and bovine oxidases originates largely, although not exclusively, in the much slower (500−1000-fold) rate of Ca^{2+} dissociation from the binding site in the *R. sphaeroides* enzyme. The structural reasons for these differences in the binding energy and kinetics are difficult to deduce at this time. The bovine oxidase crystals contain Na^+ and not Ca^{2+} (*13*) and the bacterial oxidases studied are mutants whose structures have not been determined.

The presence of one extra protein ligand to Ca^{2+} (H_2O/D485) can further increase the intrinsic affinity of the site for Ca^{2+} in the WT *R. sphaeroides* enzyme, relative to that of D485A, bringing K_d from 6 nM to subnanomolar range. Consequently, Ca^{2+} dissociation upon addition of excess EGTA could decelerate from tens of minutes in D485A to hours in the WT oxidase. Thus, thermodynamic equilibrium parameters could be sufficient to explain the apparently "irreversible" binding of the cation with the WT *R. sphaeroides* enzyme. However, such arguments are less plausible in the case of *P. denitrificans* COX, in which affinity for Ca^{2+} of the D477A mutant is about 200-fold lower than that for the *R. sphaeroides* D485A enzyme. Therefore, we propose that Ca^{2+} caging within the site (i.e., hindered equilibration with the aqueous phase), is also important for the "tight" "irreversible" binding of the cation with the bacterial oxidases in addition to the high intrinsic affinity of the site for the ligand.

Specific Role of the Aspartic Residue in Locking Ca^{2+} in the Binding Site. Ca^{2+} is coordinated by six oxygen atoms within the binding site in the *P. denitrificans* COX (*25*) and in the highly homologous *R. sphaeroides* enzyme (Figure 2). Our data confirm the critical role of the "remote" aspartate residue (D485 in *R. spaeroides*, D477 in *P. denitrificans*) in locking Ca^{2+} within the binding site in bacterial oxidases (*25*). Mutations in other residues directly coordinated to Ca^{2+} within the site, such as Q61 (Q63 in *P. denitrificans*) do not result in Ca^{2+} release from the enzyme. The unique role of the D485 (D477) residue in the "tight binding" of calcium may suggest that this residue blocks the exit pathway for Ca^{2+} from the binding domain, trapping the cation in the site.

Scheme 1: Possible Mechanism of Ca^{2+} Binding and Dissociation from the D485A Mutant from of Cytochrome c Oxidase from *R. Sphaeroides*

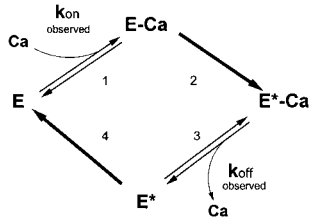

Riistama et al. (*39*) reported a Ca^{2+}-induced red shift of heme *a* in the Q63 and E54 mutants of the *P. denitrificans* oxidase, implying that these mutants lacked the endogenous Ca^{2+}. However, independent work (*25*) on the mutants in the same residues, one of which (Q63A) is identical to that used in ref *39*, showed that the tightly bound Ca^{2+} is retained, consistent with the current results with the *R. sphaeroides* oxidase. Moreover, no Ca^{2+}-induced red shift could be observed in our hands with the Q63A mutant COX from *P. denitrificans* (A.Kirichenko, unpublished). A possibility of differences between the preparations as obtained in different laboratories cannot be excluded. Notably, the affinity of the *P. denitrificans* E56Q COX mutant for Ca^{2+} reported by Riistama et al. (*39*) ($K_d \sim$ ca. 0.1 mM) is very low as compared to that found for the D477A *P. denitrificans* mutant ($K_d \sim 1$ μM) (*25*), the *R. sphaeroides* D485A mutant ($K_d \sim$ 6 nM, this work) or bovine COX. It is not clear whether this low affinity is a specific feature of the E56Q mutant or whether it indicates a major contribution of the conserved glutamate to the free energy of Ca^{2+} binding at the site.

Discrepancy between the K_d Values as Determined by Equilibrium Titrations and by Measurements of Rate Constants. Is Ca^{2+} Binding a Multistep Process? For a simple single-step reaction of Ca^{2+} binding, the equilibrium constant, K_d, must be equal to the ratio of the rate constants: $K_d = k_{off}/k_{on}$. However, the equilibrium K_d for Ca^{2+} binding with the D485A mutant (6 nM) is about 30-fold lower than the ratio of the k_{off}/k_{on} ratio (190 nM). This discrepancy may indicate that the on and off rate constants experimentally measured in this work refer to partial reactions that do not fully describe the Ca^{2+} reaction with the enzyme. An example of a possible mechanism of Ca^{2+} interaction with bacterial COX that will be consistent with the current data is shown in Scheme 1.

Note that a simple linear two-step binding scheme, E + Ca ↔ (E—Ca) ↔ E*—Ca, will not account for the data. Scheme 1 implies the initial spectrophotometrically detectable reversible binding of the cation to the enzyme (step 1) to be followed by spectrally silent protein conformational changes (step 2, E → E—Ca*). Also the unusually slow on-rates and off-rates for Ca^{2+} binding to the oxidase (both mammalian and bacterial), as compared to other Ca^{2+} binding proteins, are consistent with a multistep reaction requiring some protein structural rearrangement. This rearrangement may be confined to the cation binding site itself, as there are no indications of a gross conformational changes in COX.

Spectral Perturbation of Heme a is Induced by Ca^{2+} Binding to the Cation-Binding Site Revealed in the X-Ray Structures. The ability to bind Ca^{2+} reversibly, as revealed by direct metal content measurements, correlates with the red shift of the absorption spectrum of heme *a* in the *R. sphaeroides* oxidase mutants (Table 1). It is clear that the spectral shift induced by Ca^{2+} must be associated with binding of the cation to the site resolved by the X-ray structure of the enzyme. This is also the conclusion of previous mutagenesis studies on *the P. denitrificans* mutants despite certain discrepancies between the published studies (*25*, *39*).

Competition between Ca^{2+} and Na^+ Suggests the Identity of the Second Na^+-Binding Site in Bovine COX. In bovine COX, Na^+ competes with Ca^{2+} for binding to the enzyme, but the binding of Na^+ does not itself induce the spectral shift of heme *a* (*21*, *22*). Competition between Ca^{2+} and Na^+ has also been demonstrated recently for the *P. denitrificans* oxidase with mutations in the cation-binding site (*25*, *39*). Specific competition between Na^+ and Ca^{2+} ions for binding with the D485A mutant is revealed in this work as well. The kinetic measurements suggest that Na^+ lowers the apparent affinity of COX for calcium by decreasing the rate of Ca^{2+} binding. At 0.3 mM Ca^{2+}, 100-fold inhibition of the binding rate is obtained with 25 mM Na^+, indicating that the Na^+ affinity (K_d) of the enzyme may be in the range of 0.25 mM (i.e., 1% of the enzyme is free to bind Ca^{2+} in the presence of 25 mM Na^+).

In bovine COX, one Ca^{2+} competes with two Na^+ ions (*22*) for binding to the enzyme. This complies with charge balance but raises question as to the nature of the two sodium binding sites. One sodium ion is presumed to be coordinated in the same site as Ca^{2+} (*13*), but the identity of the second site remained obscure. The current data may provide a hint to the solution of this question. Protein-bound Ca^{2+} typically requires two carboxylates in the coordination sphere for charge neutralization. For instance, a so-called "proximal" cation binding loop in different homologous peroxidases can be empty (yeast mitochondrial cytochrome *c* peroxidase) or bind K^+ (ascorbate peroxidase) or Ca^{2+} (e.g., peanut peroxidase) in accordance with the presence of zero, one, or two aspartate residues in this domain (see ref *35* and references therein). In COX, the two carboxylates are provided by a glutamate residue (E54 in *R. sphaeroides*, E56 in *P. denitrificans*, E40 in bovine COX) and an aspartate residue (D485 in *R. sphaeroides*, D477 in *P. denitrificans*, D442 in bovine COX). In the bovine COX, one Na^+ is at the cation binding site, coordinated to E40, S441, carbonyl functions of Q43 and G45, and a water molecule, while according to ref *13*, the D442 carboxylate is free. It is tempting to suggest that the D442 carboxylate provides the second, lower-affinity binding site for Na^+ in bovine COX. Conceivably, Na^+ binding with this group in bovine oxidase will counteract Ca^{2+} binding, since coordination of the Ca^{2+} should require the presence of the second carboxylate group (D442). This suggestion is consistent with the present data indicating that Ca^{2+} competes with only one sodium ion in the *R. sphaeroides* D485A mutant, i.e., one Na^+ binding site appears to be lost concurrently with the replacement of D485 by alanine.

Possible Functional Role of the Cation-Binding Site in the Bacterial and Mitochondrial Cytochrome c Oxidases. The physiological significance of the cation-binding site in mammalian and bacterial COX remains to be established. Ca^{2+} is involved in regulation of a vast number of intracellular biochemical processes (*57*, *58*) and, in particular, enhances oxidative phosphorylation, stimulating both the respiratory and phosphorylation components of the system (see refs *59* and *60* and references therein). It is tempting to propose that the reversible binding of Ca^{2+} to the bovine oxidase may be involved in physiological regulation of respiration and energy transduction. It is worthwhile to discuss some potential venues of research of cytochrome oxidase as a Ca^{2+}-binding protein, for which the bacterial oxidase Ca^{2+}-binding mutants may serve as a useful model.

Intracellular effects of Ca^{2+} are mediated by a family of Ca^{2+} binding "trigger" proteins that change their affinity for protein/membrane targets upon Ca^{2+} binding (*57*, *58*, *61*, *62*). The K_d of 10^{-6} M for reversible Ca^{2+} binding to bovine COX (*22*) is within the $10^{-9}-10^{-5}$ M range characteristic of the intracellular Ca^{2+}-regulated trigger proteins such as calmodulins or annexins (*58*, *61*). The structure of the COX Ca^{2+}-binding site, with one ligand (H_2O/D485) supplied by a part of the amino acid sequence far removed from the main binding sequence, corresponds to the class II sites found often in many hydrolytic enzymes (*63*) and has no obvious direct homology with the classical EF-hand. It is unlikely that large scale conformational changes of COX subunit I, analogous to those in calmodulins or annexins, can be induced by Ca^{2+} binding.

The enzymatic function of COX would be the first obvious target of calcium/sodium regulation. However, no effects Ca^{2+} or Na^+ on the electron transfer or proton pumping activities of cytochrome oxidase have been firmly established so far (*18*, *22*). As proposed in (*22*), the Ca^{2+}-binding site in bovine oxidase may be involved in regulation of the exit of the putative tramsmembrane proton conducting network (*13*) (protonic H− channel, *41*; "pore A" in ref *11*) via interaction with the nearby asp-51 residue. This aspartate (bovine D51) undergoes a redox-linked conformational change in bovine COX (*13*) and is hydrogen bonded to the hydroxyl of Ser-441, which, simultaneously, coordinates Na^+ (and presumably Ca^{2+}) with its peptide carbonyl. The concerted phylogenetic appearance of the residues homologous to Ser-441 and Asp-51 of COX subunit I in the *Echinodermata* has been pointed out in (*64*) and may correlate with the appearance of hormonal regulation. While the role of the H-channel in proton pumping is not supported by mutagenesis studies on the bacterial oxidases (*45*, *65*), an interesting alternative is that in the mammalian COX, the H-channel may serve to conduct protons in the reverse direction forming a $\Delta\mu_{H^+}$ dissipating pathway. This would be a form of regulated attenuation of protonic potential (see ref *66* for a review on physiogical uncoupling), i.e., a built-in controlled uncoupling device within mammalian COX subunit I regulated by Ca^{2+} and Na^+.

Second, a possibility cannot be excluded that COX transmits the regulatory effect of Ca^{2+} to other mitochondrial proteins. Such a "passive" function of COX in the signal transduction pathway can make sense, since COX is an abundant protein in the mitochondrial membrane. Interestingly, another abundant oxidative phosphorylation enzyme, the mitochondrial ATP-synthase, also contains a Ca^{2+}-binding site located, as in COX, at the outer face of the inner

mitochondrial membrane (*67*). The Ca^{2+}-binding site of the ATP-synthase is localized in subunit *c* of the enzyme, is homologous to the Ca^{2+}-binding domain of troponin and may be part of a cGMP-stimulated voltage-sensitive cation pore inhibited by Ca^{2+} with cGMP-dependent K_d in the range of 0.1−100 μM (*68*).

Third, it is noted that the residue S441 adjacent to D442 at the Ca^{2+}/Na^+ binding site in the bovine oxidase is part of a consensus target sequence for cAMP-dependent phosphorylation ($RRYS_{441}$). Residue S441 is also a ligand to Na^+ in the crystal structure of the cation-binding site of bovine COX (*13*) and is specifically present in the cation-binding site of animal, but not plant, yeast or bacterial COX (*22*, *64*). S441 has been proposed recently to be involved in cAMP-dependent phosphorylation of the oxidase in animal mitochondria (*64*, *69*) associated with modulation of COX activity and the effectiveness of proton pumping (*64*, *69*, *70* and references therein). If phosphorylation of S441 is confirmed experimentally, this finding may provide a clue to the functional role of the $Ca^{2+}/Na^+/H^+$-specific cation-binding site in the mammalian cytochrome oxidase and reveal new, important aspects of physiological regulation of the oxidase activity in the cell.

In the two bacterial oxidases studied from *R. sphaeroides* and *P. denitrificans*, Ca^{2+} is tightly bound and not exchangeable, although it cannot be excluded that in some other bacterial cytochrome *c* oxidases reversible binding of Ca^{2+} may be found. The most obvious potential function of the tightly bound Ca^{2+} in this case is to stabilize the protein structure (e.g., *39*). In particular, Ca^{2+} may help to hold together two separate domains of COX as it binds simultaneously to ligands from the helix I−II loop and via the fixed water to D477 (D485) from the helix XI-XII loop. Decreased stability of the D485A mutant is indicated by the spontaneous time-dependent absorption changes (mainly, loss of heme *a* band) observed with both the half-reduced (e.g., Figure 6B) or oxidized (not shown) mutant enzyme. Notably, this instability is not affected significantly by Ca^{2+}. The spontaneous changes are essentially the same either in the presence of EGTA or Ca^{2+}. This is not an unexpected result, since in the absence of a D485 residue, Ca^{2+} will not be able to bridge the helix I−II and helix XI-XII domains and, even when bound to the site, may not reveal its stabilizing function.

ACKNOWLEDGMENT

Thanks are due to Drs. S. Iwata and P. Brzezinski for providing the 3D structure of COX from *R. sphaeroides.* We are obliged to Dr. J. Morgan for his kind help in the rapid kinetics experiments, to Prof. A. Vinogradov for valuable discussion, and to Prof. B. Kadenbach for providing a manuscript of his paper (*64*) prior to publication.

REFERENCES

1. Babcock, G. T., and Wikström, M. (1992) *Nature 356*, 301−309.
2. Ferguson-Miller, S., and Babcock, G. T. (1996) *Chem. Rev. 7*, 2889−2907.
3. Michel, H., Behr, J., Harrenga, A., and Kannt, A. (1998) *Annu. Rev. Biophys. Biomol. Struct. 27*, 329−356.
4. Einarsdottir, O., and Caughey, W. (1985) *Biochem. Biophys. Res. Commun. 129*, 840−847.
5. Bombelka, E., Richter, F.-W., Stroh, A., and Kadenbach, B. (1986) *Biochem. Biophys. Res. Commun. 140*, 1007−1014.
6. Steffens, G. C. M., Biewald, R., and Buse, G. (1987) *Eur. J. Biochem. 164*, 295−300.
7. Moubarak, A., Pan, L. P., and Millet, F. (1987) *Biochem. Biophys. Res. Commun. 143*, 1030−1036.
8. Steffens, G. C. M., Soulimane, T., Wolff, G., and Buse, G. (1993) *Eur. J. Biochem. 213*, 1149−1157.
9. Tsukihara, T., Aoyama, H., Yamashita, E., Tomizaki, T., Yamaguchi, H., Shinzawa-Itoh, K., Nakashima, T., Yaono, R., and Yoshikawa, S. (1995) *Science 269*, 1069−1074.
10. Tsukihara, T., Aoyama, H., Yamashita, E., Takashi, T., Yamaguichi, H., Shinzawa-Itoh, K., Nakashima, R., Yaono, R., and Yoshikawa, S. (1996) *Science 272*, 1136−1144.
11. Iwata, S., Ostermeier, C., Ludwig, B., and Michel, H. (1995) *Nature 376*, 660−669.
12. Ostermeier, C., Harrenga, A., Ermler, U., and Michel, H. (1997) *Proc. Natl. Acad. Sci. U.S.A. 94*, 10547−10553.
13. Yoshikawa, S., Shinzawa-Itoh, K., Nakashima, R., Yaono, R., Inoue, N., Yao, M., Fei, M. J., Libeu, C. P., Mizushima, T., Yamaguchi, H., Tomizaki, T., and Tsukihara, T. (1998) *Science 280*, 1723−1729.
14. Hosler, J. P., Espe, M. P., Zhen, Y., Babcock, G. T., and Ferguson-Miller, S. (1995) *Biochemistry 34*, 7586−7592.
15. Witt, H., Witterschagen, A., Bill, E., Kolbesen, B. O., and Ludwig, B. (1997) *FEBS Lett. 409*, 128−130.
16. Florens, L., Hoganson, C., McCracken, J., Fetter, J., Mills, D., Babcock, G. T., and Ferguson-Miller, S. (1999) in *The Photosynthetic Procaryotes* (Peschek, G. E. A., Ed.) pp 329−339, Kluwer Academic/Plenum Publishers, New York.
17. Wikstrom, M., and Saari, H. (1975) *Biochim. Biophys. Acta 408*, 170−179.
18. Saari, H., Pentilla, T., and Wikstrom, M. (1980) *J. Bioenerget. Biomembr. 12*, 325−338.
19. Nicholls, P. (1975) *Biochim. Biophys. Acta 396*, 24−35.
20. Konstantinov, A., Vygodina, T., Popova, E., Berka, V., and Musatov, A. (1989) *FEBS Lett. 245*, 39−42.
21. Mkrtchyan, H., Vygodina, T., and Konstantinov, A. A. (1990) *Biochem. Int. 20*, 183−190.
22. Kirichenko, A., Vygodina, T. V., Mkrtchyan, H. M., and Konstantinov, A. A. (1998) *FEBS Lett. 423*, 329−333.
23. Abramson, J., Riistama, S., Larsson, G., Jasaitis, A., Svensson-Ek, M., Laakkonen, L., Puuustinen, A., Iwata, S., and Wikstrom, M. (2000) *Nat. Struct. Biol. 7*, 910−917.
24. Soulimane, T., Buse, G., Bourenkov, G. B., Bartunik, H. D., Huber, R., and Than, M. E. (2000) *EMBO J. 19*, 1766−1776.
25. Pfitzner, U., Kirichenko, A., Konstantinov, A. A., Mertens, M., Wittershagen, A., Kolbesen, B. O., Steffens, G. C. M., Harrenga, A., Michel, H., and Ludwig, B. (1999) *FEBS Lett. 456*, 365−369.
26. Booth, K. S., Kimura, S., Lee, H. C., Ikeda-Saito, M., and Caughey, W. S. (1989) *Biochem. Biophys. Res. Commun. 160*, 897−902.
27. Zeng, J., and Fenna, R. E. (1992) *J. Mol. Biol. 226*, 185−207.
28. Shin, K., Hayasawa, H., and Lonnerdal, B. (2001) *Biochem. Biophys. Res. Commun. 281*, 1029−1029.
29. Gilmour, R., Goodhew, C. F., Pettigrew, G. W., Prazeres, S., Moura, I., and Moura, J. J. G. (1993) *Biochem. J. 294*, 745−752.
30. Prazeres, S., Moura, J. J. G., Moura, I., Gilmour, R., Goodhew, C. F., Pettigrew, G. W., Ravi, N., and Huynh, B. H. (1995) *J. Biol. Chem. 270*, 24264−24269.
31. Sundaramoorthy, M., Kishi, K., Gold, M. H., and Poulos, T. L. (1994) *J. Biol. Chem. 269*, 32759−32767.
32. Kunishima, N., Fukuyama, K., Matsubara, H., Hatanaka, H., Shibano, Y., and Amachi, T. (1994) *J. Mol. Biol. 235*, 331−344.
33. Sutherland, G. R. J., Zapanta, L. S., Tien, M., and Aust, S. D. (1997) *Biochemistry 36*, 3654−3662.
34. Barber, K. R., Rodriguez Maranon, M. J., Shaw, G. S., and van Huystee, R. B. (1995) *Eur. J. Biochem. 232*, 825−833.
35. Schuller, D. J., Ban, N., van Huystee, R. B., McPherson, A., and Poulos, T. L. (1996) *Structure 4*, 311−321.
36. Zhao, D., Gilfoyle, D. J., Smith, A. T., and Loew, G. H. (1996) *Proteins 26*, 204−216.
37. Rasmussen, C. B., Hiner, A. N. P., Smith, A. T., and Welinder, K. G. (1998) *J. Biol. Chem. 273*, 2232−2240.
38. Vrettos, J. S., Limburg, J., and Brudvig, G. W. (2001) *Biochim. Biophys. Acta 1503*, 229−245.
39. Riistama, S., Laakkonen, L., Wikstrom, M., Verkhovsky, M. I., and Puustinen, A. (1999) *Biochemistry 38*, 10670−10677.
40. Brzezinski, P., and Adelroth, P. (1998) *J. Bioenerget. Biomembr. 30*, 99−107.
41. Gennis, R. B. (1998) *Biochim. Biophys. Acta 1365*, 241−248.

42. Fetter, J. R., Qian, J., Shapleigh, J., Thomas, J. W., Garcia-Horsman, A., Schmidt, E., Hosler, J., Babcock, G. T., Gennis, R. B., and Ferguson-Miller, S. (1995) *Proc. Natl. Acad. Sci. U.S.A. 92*, 1604−1608.
43. Mitchell, D. M., and Gennis, R. B. (1995) *FEBS Lett. 368*, 148−150.
44. Dawson, R. M. C., Elliott, D. C., Elliott, W. H., and Jones, K. M. (1986) *Data for Biochemical Research*, 3rd ed., Clarendon Press, Oxford.
45. Lee, H.-m., Das, T. K., Rousseau, D. L., Mills, D., Fergusson-Miller, S., and Gennis, R. (2000) *Biochemistry 39*, 2989−2996.
46. Zaslavsky, D., Kaulen, A., Smirnova, I. A., Vygodina, T. V., and Konstantinov, A. A. (1993) *FEBS Lett. 336*, 389−393.
47. Konstantinov, A. A., Siletskiy, S. A., Mitchell, D., Kaulen, A. D., and Gennis, R. B. (1997) *Proc. Natl. Acad. Sci. U.S.A. 94*, 9085−9090.
48. Siletsky, S., Kaulen, A. D., and Konstantinov, A. A. (1999) *Biochemistry 38*, 4853−4861.
49. Nilsson, T. (1992) *Proc. Natl. Acad. Sci. U.S.A. 89*, 6497−6501.
50. Vygodina, T., Konstantinov, A., Kirichenko, A., Mkrtchan, H., and Musatov, A. (1995) Abstracts of the 23th FEBS Meeting, Basel, Switzerland, p 348.
51. Kirichenko, A. (1995) Masters Thesis, M. V. Lomonosov Moscow State University, Moscow.
52. Johnson, J. D., Snyder, C., Walsh, M., and Flynn, M. (1996) *J. Biol. Chem. 271*, 761−767.
53. Fast, J., Hakansson, M., Muranayi, A., Gippert, G. P., Thulin, E., Evenas, J., Svensson, L. A., and Linse, S. (2001) *Biochemistry 40*, 9887−9895.
54. Drachev, L. A., Kaulen, A. D., and Khitrina, L. V. (1988) *Biochemistry (Moscow) 53*, 663−667.
55. Varo, G., Brown, L. S., Needleman, R., and Lanyi, J. K. (1999) *Biophys. J. 76*, 3219−3226.
56. Keller, S., Beatty, J. T., Paddock, M., Breton, J., and Leibl, W. (2001) *Biochemistry 40*, 429−439.
57. Clapham, D. E. (1995) *Cell 80*, 259−268.
58. Evenas, J., Malmendal, A., and Forsen, S. (1998) *Curr. Opin. Chem. Biol. 2*, 293−302.
59. Mildaziene, V., Baniene, R., Naugiene, Z., Marcinkeviciute, A., Morkuniene, R., Borutaite, V., Kholodenko, B., and Brown, G. (1996) *Biochem. J. 320*, 329−334.
60. Jouville, L. S., Pinton, P., Bastianutto, C., Rutter, G. A., and Rizzuto, R. (1999) *Proc. Natl. Acad. Sci. U.S.A. 96*, 13807−13812.
61. Forsen, S., and Kordel, J. (1991) in *Bioinorganic Chemistry* (Bertini, I., Gray, H. B., Lippard, S. J., & Valentine, J. S., Eds.) pp 107−166, University Science Books, Mill Valley.
62. Berridge, M. J., Lipp, P., and Bootman, M. D. (2000) *Nat. Rev. Mol. Cell Biol. 1*, 11−21.
63. Pidcock, E., and Moore, G. R. (2001) *J. Biol. Inorg. Chem. 6*, 479−489.
64. Lee, I., Bender, E., Arnold, S., and Kadenbach, B. (2001) *Biol. Chem. 382*, 1629−1636
65. Pfitzner, U., Odenwald, A., T. ., O., Weingard, L., Ludwig, B., and Richter, O. M. (1998) *J. Bioenerget. Biomembr. 30*, 89−97.
66. Skulachev, V. P. (1999) *J. Bioenerget. Biomembr. 31*, 431−445.
67. Akaraku, N., Ueyama, Y., Hirose, M., Himeda, T., Shibata, H., Futaki, S., Kitagawa, K., and Higuti, T. (2001) *Biochim. Biophys. Acta 1504*, 220−228.
68. McGeoch, J. E. M., McGeoch, M. W., Mao, R., and Guidotti, G. (2000) *Biochem. Biophys. Res. Commun. 274*, 835−840.
69. Ludwig, B., Bender, E., Arnold, S., Huttemann, M., Lee, I., and Kadenbach, B. (2001) *ChemBioChem 2*, 392−403.
70. Bender, E., and Kadenbach, B. (2000) *FEBS Lett. 466*, 130−134.

BI020183X